

# The Transport of Tyrosine into the Human Brain as Determined with L-[1-<sup>11</sup>C]Tyrosine and PET

Frits-Axel Wiesel, Gunnar Blomqvist, Christer Halldin, Irene Sjögren, Lars Bjerkenstedt, Nikolaos Venizelos, and Lars Hagenfeldt

*Department of Psychiatry, University of Uppsala, Sweden and Departments of Clinical Neurophysiology Psychiatry and Psychology, and Clinical Chemistry, Karolinska Institute, Stockholm, Sweden*

An alteration of dopaminergic transmission in the brain has been proposed for schizophrenia. To explore this, the rate constant for the intransport of L-tyrosine across the blood-brain barrier in healthy controls and in patients with schizophrenia (DSM-III-R) was determined with PET and L-[1-<sup>11</sup>C]tyrosine as the tracer. Kinetics for tyrosine transport were determined according to a two-compartment model using radioactivity data of arterial blood and brain tissue sampled between 1 and 3.5 min after a bolus injection of L-[1-<sup>11</sup>C]tyrosine. Radioactivity was measured every second in the blood and in 10-sec intervals in the brain tissue. In the normal controls the brain intransport rate constant for tyrosine was 0.052 ml/g/min with an influx rate of 2.97 nmol/g/min. The patients had a similar intransport rate constant (0.045 ml/g/min) but a lower influx rate of tyrosine 1.95 nmol/g/min ( $p < 0.05$ ). The patients' tyrosine concentrations in the blood were lower. For data sampled between 5 and 25 min, the net accumulation rate of tyrosine into the brain was 0.015 ml/g/min in the controls which did not differ to the patients' rate. However, the net utilization of tyrosine was lower in the patients (0.672 nmol/g/min) than in the controls (0.883 nmol/g/min) despite similar tissue concentrations of tyrosine.

J Nucl Med 1991; 32:2043–2049

mechanisms. Recently it was found that the transport of L-tyrosine in vitro in cultured fibroblasts from schizophrenic patients was decreased which may indicate that a change in the availability of precursor to dopamine, may be one factor in the pathophysiology of schizophrenia (10). The in vitro findings demonstrated an isolated decrease in the transport capacity ( $V_{max}$ ) for L-tyrosine. The  $K_m$  for L-tyrosine transport was unaffected. The competitive inhibition among the amino acids transported by the L-system was normal in the cells from the patients. It was concluded that the in vitro decrease of L-tyrosine transport into the cells could not be related to any known transport system of amino acids. The in vitro findings motivated us to determine the transport of L-tyrosine in vivo into the brain in healthy volunteers and in patients with schizophrenia. This was performed with PET and L-[1-<sup>11</sup>C]tyrosine as the tracer. The intransport rate constant ( $k_1$ ) was determined in a two-compartment model from data sampled during the first 4 min after the injection of the tracer. Regional cerebral blood volume was determined by using [<sup>11</sup>C]CO-hemoglobin. The complexity of the studies restricted the number of normals and patients investigated.

## MATERIALS AND METHODS

The study was approved by the Ethics Committee and the Committee of Radiation Safety of the Karolinska Hospital. Five healthy male volunteers were selected for the study. The volunteers were examined clinically to exclude those with previous or actual psychiatric disturbances, as well as subjects with prior head injury or infection of the central nervous system, systemic or neurologic diseases. None of the healthy volunteers had previous or ongoing abuse of alcohol or narcotics of any kind. Male psychotic patients ( $n = 5$ ) without neuroleptic treatment who were admitted to the psychiatric emergency unit at the Karolinska Hospital were selected for the study (Table 1). The patients had to fulfill the DSM-III-R criteria of schizophrenia for inclusion in the study. Patients with organic brain disorder, somatic disease, prior head injury or infection of the central nervous system, or previous or ongoing abuse of alcohol or narcotics were excluded. Both patients and volunteers underwent a physical examination and an analysis of blood chemistry reflecting liver, kidney and blood function was performed. No abnormalities were found.

The controls and the patients had the same PET protocol for determination of tyrosine transport across the blood-brain barrier.

Tyrosine is the precursor amino acid of brain noradrenaline and dopamine synthesis. In the transport of tyrosine across the blood-brain barrier, the L-system is used in competition with other neutral amino acids (1–4). In humans the transport of tyrosine into the brain has so far only been estimated relative to the other neutral amino acids in plasma (5,6). However, positron emission tomography (PET) makes it possible to directly quantify L-tyrosine transport.

The transport of tyrosine is of special interest to schizophrenia research since an alteration of dopaminergic transmission in the brain has been proposed (7–9). Support for this hypothesis originates from the effects of neuroleptics and amphetamine on central dopaminergic

Received Dec. 7, 1990; revision accepted Jul. 11, 1991.

For reprints contact: Frits-Axel Wiesel, MD, PhD, Department of Psychiatry, Uppsala University, Ulleråker, S-750 17 Uppsala, Sweden.

**TABLE 1**  
Clinical Characteristics of the Patients with Schizophrenia

Age (yr)	Subtype	Duration of the disease (yr)	Last psychotropic- medication prior to PET (yr)	Psychiatric morbidity in the family
32	Disorganized	5	4.5	+
31	Disorganized	8	0.5	-
33	Undifferentiated	5	0.7	-
18	Disorganized	0.7	never medicated	-
27	Disorganized	1	never medicated	+

Diagnosis was made according to DSM-III-R. The patients were admitted to the hospital to obtain treatment for their psychotic symptoms. According to anamnestic information obtained from patients and relatives, no patient had taken neuroleptics within 6 mo before entering the hospital. The patients were inpatients without drug treatment ~2 wk prior to PET investigations. The controls were five healthy men aged 22, 24, 26, 27 and 28 yr.

The subjects fasted for 15 hr (water intake 12 hr) before the PET experiment, which started at 11 a.m. During that period of time, the subjects, postabsorptive levels of amino acids in plasma were determined by the net balance between release and uptake from different endogenous stores.

Volunteers and patients were all examined by computed tomography (CT) of the brain. To allow identical positioning in the CT and PET scan examinations, a special head positioning device was used (11). Displayed CT images of each subject were used to identify brain regions of interest. Cortical regions were approximately delineated according to Brodmann areas (12). Centrally located structures and nuclei were drawn according to the anatomical boundaries seen on the CT images. A region was drawn only at one slice level. At each slice level, the circumference of the brain surface was delineated to calculate the total transport of tyrosine into the brain and the total brain blood volume. Whole brain volume included ventricular spaces. In each subject, the foramen of Monro was identified with CT and the brain was positioned so that the middle of PET section number four was 3 mm above the foramen. The marked regions were automatically transferred to the corresponding slice levels of the PET examinations to determine the transport of tyrosine and the blood volume.

DL-[1-<sup>11</sup>C]tyrosine was prepared by use of the Bücherer-Strecker reaction, from carrier-added <sup>11</sup>C-cyanide with an incorporation of 80% in 20 min (13). The isolation of the pure D- and L-amino acid isomers from the enantiomeric mixture was accomplished within 15 min by semi-preparative high-performance liquid chromatography (HPLC) using a chiral stationary phase and a phosphate buffer as the mobile phase. A carrier-added specific activity of 0.3–0.5 Ci/mmol was obtained and a radiochemical purity better than 99%. L-[1-<sup>11</sup>C]tyrosine 150–325 MBq was injected intravenously as a bolus. The radioactivity in the brain was measured with a four-ring positron camera (PC-384-7B) (FWHM = 7.6 mm) in 3.5 min (20 scans of 10 sec duration). Eleven additional scans were made during the following 20 min. Blood samples were taken from the brachial artery of the contralateral arm. The concentrations of unlabeled tyrosine were determined immediately before and during the PET investigation (14). The levels were almost identical. During the first

3.5 min, an automatic blood sampling system (ABSS) was used (15,16). The ABSS consisted of a long catheter, a detector to measure the concentration of the radioactivity in the catheter and a peristaltic pump to draw arterial blood into the catheter. The pump speed was set to 5 ml/min. The detector system was connected to a microprocessor, and the concentration of radioactivity in the catheter was measured and stored every second. From the open end of the catheter, six blood samples (1.0 ml) were taken during the 3.5 min period after the injection. These samples were used for calibration of the ABSS. The difference in time between manual and automatical blood sampling was taken into account in the calculations. Data from the ABSS and the total count rate from the positron camera were transferred to the computer and the time shift between the arterial blood curve and the total brain uptake curve was determined and used to adjust the measuring time. Use of the ABSS implies a certain dispersion (broadening) of the blood curve. This distortion affects the value of the influx rate constant  $k_1$  (see Results). When L-[1-<sup>11</sup>C]tyrosine data were corrected for dispersion, the  $k_1$  values changed by 3% (15). This small effect has not been taken into account in the present study. After the first 3.5 min, arterial blood samples (2 ml) were collected from the open end of the catheter at each scan until the end of the experiment. One millimeter of the manually collected samples was immediately pipetted and measured for 10 sec in a well counter. After centrifugation, 0.2 ml of plasma was pipetted and plasma radioactivity was also measured in the well counter.

Regional cerebral blood volume was determined by using [<sup>11</sup>C]CO-hemoglobin which was synthesized by trapping [<sup>11</sup>C]carbon monoxide in a 10-ml suspension of sterile saline and red blood cells of the subjects (17). Before injection of [<sup>11</sup>C]CO-hemoglobin, radioactivity background radioactivity was determined in one scan (5 min). The injection was always performed at least five half-lives of <sup>11</sup>C after the L-[1-<sup>11</sup>C]tyrosine injection. PET measurements started 5 min after the injection of [<sup>11</sup>C]CO-hemoglobin and lasted for 20 min in a series of 2-min scans. Six arterial blood samples were taken to calibrate the ABSS to the well counter and the camera.

Regional cerebral blood volume was calculated according to the method by Phelps (18) after subtraction of the background radioactivity. Cerebral blood volume data were then used in the calculation of tyrosine transport and the accumulation of radioactivity in brain tissue.

### Theory

We assumed that the transport of tyrosine across the blood-brain barrier could be described with the Michaelis-Menten equation:

$$I = \frac{C_a \cdot V_{max}}{C_a + K_m}, \quad \text{Eq. 1}$$

where  $I$  = the influx rate and  $C_a$  = the tyrosine concentration in arterial plasma (nmol/ml). The influx of tyrosine was also related to  $C_c$ , the average capillary concentration of tyrosine, and  $P_iS$ , the permeability surface area product, by the equation:

$$I = C_c \cdot P_iS \quad \text{Eq. 2}$$

The fractional extraction of amino acids was low and their clearance through the brain is diffusion-limited and flow-independent at normal rates of cerebral blood flow (CBF) (19,20),

which implied:

$$C_c \approx C_a \quad \text{Eq. 3}$$

According to Crone (21), the following equation is valid:

$$k_1 = \text{CBF} \cdot (1 - e^{-PIS/CBF}), \quad \text{Eq. 4}$$

where  $k_1$  is the rate constant of the intransport. Since  $PIS \ll CBF$ ,  $k_1$  is close to  $PIS$  and the influx of tyrosine can be approximated with:

$$I = k_1 \cdot C_a; \quad \text{Eq. 5}$$

$$k_1 = \frac{V_{max}}{C_a + K_m}. \quad \text{Eq. 6}$$

The last equation implies that  $k_1$  decreases with increasing concentrations of tyrosine.

The metabolism and the incorporation of tyrosine to proteins probably occurred only to a very low extent during the first 4 min and therefore were disregarded in the calculations (22,23). We therefore assumed that there is a single compartment of L-[1-<sup>11</sup>C]tyrosine in the tissue. The exchange of tracer between plasma and tissue was described by the following differential equation:

$$\frac{dC_{tiss}^*}{dt} = k_1 C_p^* - k_2 C_t^* x_{tiss}, \quad \text{Eq. 7}$$

where  $C_{tiss}^*$  is the brain-tissue concentration,  $C_p^*$  is the arterial plasma concentration and  $k_1$  and  $k_2$  are first order rate constants.

The integration of Equation 7 gave the following operational equation:

$$C_{obs}^*(T) = CBV \cdot C_{blood}^* + k_1 \int_0^T C_p^* dt - k_2 \int_0^T (C_{obs}^* - CBV \cdot C_{blood}^*) dt, \quad \text{Eq. 8}$$

where  $C_{obs}^*$ ,  $C_{blood}^*$ ,  $C_p^*$  and  $CBV$  are measured. The two parameters  $k_1$  and  $k_2$  enter linearly in Equation 8 and are estimated by a linear least squares method (24).

The measured radioactivity between 5 and 25 min after the tracer injection was used to determine the net accumulation rate of tyrosine. The tracer will enter many pools in the tissue, but irrespective of the complexity of the processes, if there is at least one pool where the tracer is effectively trapped during the measuring time, the time course of the tracer will become simple with increasing time (25). Under general assumptions, it can be shown that the ratio of the tracer concentrations in tissue and plasma,  $C_{tiss}^*(T)/C_p^*(T)$  (Equation 9) plotted as function of the ratio of the time-integrated plasma concentration and the plasma concentration (effective time)  $\int_0^T C_p^*(t) dt / C_p^*(T)$  (Equation 10) will asymptotically approach a straight line with a slope equal to the accumulation rate of tracer. The intercept with the y-axis, the apparent volume of distribution,  $V_d$ , is lower than or equal to the physical volume of distribution of the tracer. For tracers with a very slow accumulation rate (e.g. L-[1-<sup>11</sup>C]tyrosine), the apparent  $V_d$  times the concentration of unlabeled tyrosine in the plasma,  $C_a$ , can be used as a measure of the tissue concentration of tyrosine. This method will underestimate the true tissue concentration, but our aim is not to obtain an absolute value of this quantity but to compare patients and controls.

Thus, the ratio between the concentrations of radioactivity in the brain tissue and in the plasma (y-axis in Equation 9, the

apparent volume) was plotted against the ratio between the time-integrated plasma concentration and the plasma concentration on the x-axis (Equation 10, the effective time) (see Fig. 3). A straight line was fitted to the data (Fig. 3). As loss of tracer from the tissue during the later points in time cannot be excluded (see Results), the slope represents a "net accumulation rate" of the tracer in the tissue. Multiplication of this quantity by the unlabeled plasma-tyrosine concentration yields the "net utilization rate" of tyrosine. It must be kept in mind that our aim is not to develop any exhaustive tracer kinetic model for L-[1-<sup>11</sup>C]tyrosine: instead, we will use this quantity to compare patients and controls.

## RESULTS

In Figure 1 the radioactivity following the injection of L-[1-<sup>11</sup>C]tyrosine in blood and brain is depicted. After an initial peak in brain radioactivity, there was a steady increase about 45 sec after the injection. The in- and out-transport rate constants were calculated for the data obtained between 1 and 3.5 min after the tracer injection (Table 2). Because of the short measuring time (<4 min), the measurement error of the out-transport rate constant ( $k_2$ ) was large (data not presented,  $k_2$  is rather model-dependent, so if the pool of tyrosine in the tissue was divided in two compartments, one extra- and one intracellular, the  $k_2$  parameter should change drastically, whereas the  $k_1$  parameter should be much less affected). Plasma-tyrosine concentrations were lower in patients than in the controls (Table 2). Cerebral blood volume was almost identical in the two groups. The intransport rate constant did not differ between the groups. The influx rate of tyrosine (cf. Equation 5) was significantly lower in the patients than in the controls (Table 2), since the patients' intransport constants remained low despite their lower tyrosine concentrations (Fig. 2). The intransport constant was similar among the cortical and the subcortical regions and did not differ between the controls and the patients (Table 3). Regional influx rates showed the same tendency for the whole brain but did not reach significance probably due to an increased variance of the regions (low radioactivity) and the limited number of subjects investigated (Table 3).

A Patlak plot of tyrosine is presented in Figure 3. The concavity of the late part of the curve indicates that tracer is lost from the tissue during this period of time or, alternatively, that labeled metabolites in the plasma affect the input function. The radioactivity data obtained between 5 and 25 min after the injection were fitted to a straight line. The net accumulation rate of radioactivity did not differ between the groups but the apparent volume of distribution and the net utilization of tyrosine did (Table 4). The estimated tissue concentration of tyrosine did not differ significantly between controls and patients (Table 4).

## DISCUSSION

In the rat, tyrosine is rapidly decarboxylated and 5 min after the injection of L-[1-<sup>11</sup>C]tyrosine 85% of the radio-

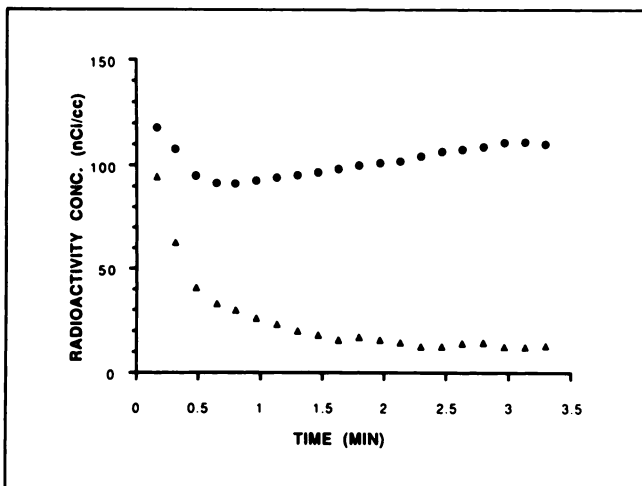


**FIGURE 1.** Radioactivity in blood times cerebral blood volume (lower points) (only the points for the mid-interval of the camera are shown) and brain (higher points) of a healthy volunteer after an intravenous injection of L-[ $^{11}\text{C}$ ]tyrosine.

activity in plasma was tyrosine and about 15% was bicarbonate and other nonprotein metabolites (22). Thirty minutes after the injection the corresponding percentages were 36% and 10%, respectively (the relative decrease in bicarbonate was suggested to reflect the formation of proteins containing tyrosine) (Idem). If these figures are relevant for man the determination of the intransport rate constant of tyrosine should be valid, but the net accumulation rates obtained from the Patlak plots are probably affected by losses of  $^{11}\text{C}$ -metabolites from the tissue. However, it should be pointed out that tyrosine turnover in

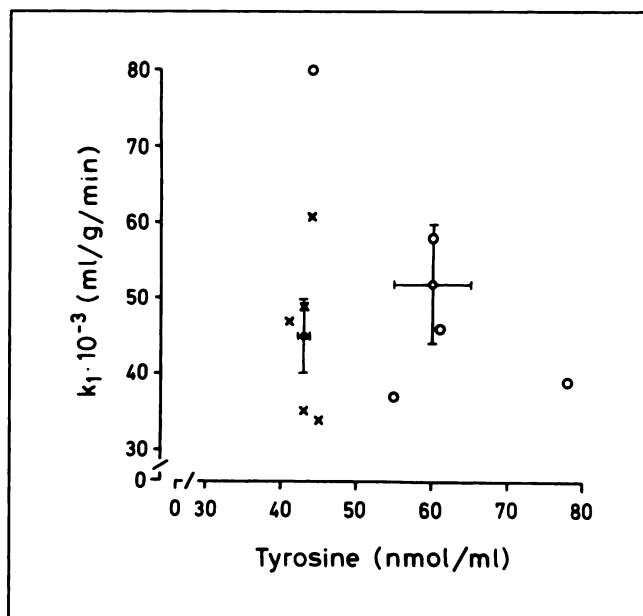


**FIGURE 2.** Concentrations of tyrosine in arterial plasma plotted versus the intransport constants for tyrosine in controls (○) and in patients (×). Mean values with their respective standard errors are drawn.

man is lower and the half-life of tyrosine has been determined to be about 3 hr using deuterium-labeled tyrosine (23).

The intransport rate constant of tyrosine for the whole brain was very similar to that found in experimental animals. Thus, in a study of the rat by Miller (26), the rate constant of nonsaturable transport of tyrosine was found to be 0.039 ml/min/g. The method used to calculate the

**TABLE 2**  
The Transport of Tyrosine from Plasma to the Whole Brain According to a Two-Compartment Model in Healthy Men and Male Schizophrenic Patients

	Tyrosine (nmol/ml)	CBV (ml/g)	$k_1$ (ml/g/min)	Influx rate ( $k_1 \cdot C_a$ ) (nmol/g/min)
Controls	60	0.040	0.058	3.47
	61	0.052	0.046	2.80
	55	0.037	0.037	2.05
	44	0.041	0.080	3.50
	78	0.045	0.039	3.02
	Mean ± s.d.	60 ± 12	0.043 ± 0.006	0.052 ± 0.018
Patients	44	0.058	0.061	2.70
	43	0.038	0.049	2.12
	45	0.038	0.034	1.52
	43	0.055	0.035	1.49
	41	0.037	0.047	1.91
	Mean ± s.d.	43 ± 1.5	0.045 ± 0.010	0.045 ± 0.011

Whole brain was made up from the five highest slice levels. Cerebellum, the inferior temporal poles, gyri recti and the vertex of the cortical surface were not included. Tyrosine kinetics were determined from data collected between 1 and 3.5 min after the tracer injection. The patients had significantly lower tyrosine concentrations and influx rates. The  $k_2$ -values ( $\text{min}^{-1}$ ) were  $0.057 \pm 0.051$  (s.d.) in the controls and  $0.020 \pm 0.035$  (s.d.) in the patients.  $C_a$  = arterial concentration of tyrosine.

\*  $p < 0.05$ . Student's t-test, two-tailed. The influx rates were decreased in all the slice levels constituting the whole brain.

**TABLE 3**  
The Regional Transport of Tyrosine Across the Blood-Brain Barrier According to a Two-Compartment Model in Healthy Men and Male Schizophrenic Patients

Brain region	$k_1$ (ml/g/min)		Influx rate ( $k_1 \cdot C_a$ ) (nmol/g/min)	
	Controls	Patients	Controls	Patients
Brodmann 10	0.046 ± 0.010	0.047 ± 0.016	2.70 ± 0.43	2.05 ± 0.74
Temporal pole	0.050 ± 0.021	0.045 ± 0.013	2.83 ± 0.77	1.93 ± 0.57
Cingulum	0.053 ± 0.02	0.057 ± 0.021	2.98 ± 0.63	2.47 ± 0.89
Caudatus	0.048 ± 0.029	0.035 ± 0.027	3.12 ± 2.62	1.51 ± 1.20
Lentiformis	0.044 ± 0.016	0.059 ± 0.021	2.59 ± 1.00	2.55 ± 0.86
Thalamus	0.061 ± 0.018	0.058 ± 0.018	3.50 ± 0.59	2.52 ± 0.83
Cerebellum	0.064 ± 0.021	0.062 ± 0.015	3.73 ± 0.99	2.67 ± 0.69

Mean ± s.d. Number of controls were five but four in the patient group since regional evaluation was not possible in one patient due to technical reasons. That patient had the lowest whole brain influx rate (1.49 nmol/g/min). No significant differences were found.

intransport of tyrosine in man, using measurements during the first 5 min after the tracer injection, seems therefore reliable. No variation of tyrosine transport between grey matter regions was evident. The similar regional intransport rate constants are probably due to the fact that the clearance of amino acids through the brain is diffusion-limited and flow-independent (19,20). Using data between 5 and 25 min after tracer injection, a net accumulation rate of 0.015 ml/min/g was found, which is very similar to that reported for methionine in man, 0.016 ml/min/g (27).

There were no differences in intransport rate constants or net accumulation rates of tyrosine (ml/g/min) between controls and patients, but the influx and the net utilization

of tyrosine (nmole/g/min) were lower for patients. The results presented in Figure 2 indicate that no single set of  $V_m$ - and  $K_m$ -values can describe the relation between  $k_1$  and  $C_a$  for both the patients and the controls. In fact, the results are in accordance with the in vitro findings showing a lower  $V_{max}$  for tyrosine across the fibroblast membrane in schizophrenic patients (24). According to Michaelis-Menten's Equation 1, one should expect the intransport rate constant to be larger for the patients due to their lower tyrosine concentrations (cf Equation 6), but this was not the case. Assuming, as found in the in vitro study, that  $K_m$  is the same for the two groups, Equation 6 yields the following relationship between the differences ( $\Delta$ ) in  $V_m$ ,

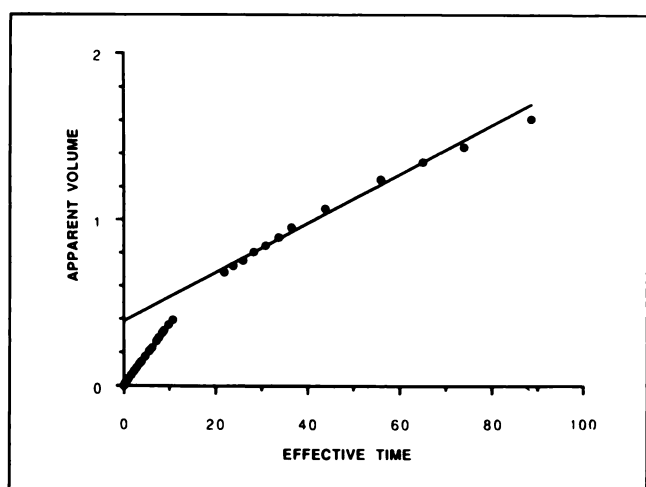


**FIGURE 3.** Apparent volume (the ratio between the concentrations of radioactivity in the brain tissue and in the plasma) in a healthy volunteer. Effective time is the ratio of radioactivity between the time-integrated plasma concentration and the plasma concentration (Equation 10). The subject with the median net accumulation rate is depicted. A straight line was fitted to data sampled between 5 and 25 min after intravenous injection of L-[1-<sup>14</sup>C]tyrosine.

**TABLE 4**  
Brain Uptake of L-[1-<sup>14</sup>C]Tyrosine in Healthy Controls and Male Schizophrenic Patients

Net accumulation rate (ml/g/min)	Virtual $V_d$ (ml/g)		Utilization of tyrosine (nmol/g/min)	
	Controls	Patients	Controls	Patients
0.0153	0.0169	0.416	0.417	0.919
0.0158	0.0158	0.314	0.401	0.961
0.0147	0.0127	0.387	0.431	0.811
0.0142	0.0167	0.397	0.412	0.626
0.0140	0.0158	0.330	0.435	1.096
Means				
0.0148	0.0156	0.369	0.419*	0.883
s.d.				
±0.0007	±0.0017	±0.044	±0.014	±0.176
				±0.066

Data obtained between 5 and 25 min after the L-[1-<sup>14</sup>C]tyrosine injection were fitted to a straight line giving the net accumulation rate and the distribution volume. All correlations were above 0.98. Utilization of substrate is the product of the net accumulation rate and the concentration of tyrosine in plasma.

\* p < 0.05. Student's t-test, two-tailed.

The tissue concentration of free tyrosine (nmol/g) was estimated to 22 ± 3.6 (s.d.) in the controls and 18 ± 0.8 (s.d.) in the patients.  $V_d$  = Volume of distribution.

I, and k<sub>i</sub> between controls and patients:

$$\Delta V_m = \Delta I + \Delta k_i \cdot K_m.$$

We have no measure of the in vivo value of K<sub>m</sub>, but in view of the in vitro value 22–27 nmol·ml<sup>-1</sup> (24), the range 10–100 nmol·ml<sup>-1</sup> is reasonable. Insertion of the measured values of I and k<sub>i</sub> (Table 2) then gives the range 1.0–1.7 nmole·g<sup>-1</sup>·min<sup>-1</sup> of difference in V<sub>m</sub> between the groups. In vitro V<sub>max</sub> was found to be 40% lower for the patients (4.5 compared to 7.8 μmol·min<sup>-1</sup>·mg<sup>-1</sup> protein). Thus, the transport of tyrosine in vivo also appears to be disturbed in patients with schizophrenia.

The observation that the lower plasma-tyrosine concentration in patients was not compensated for by an increased efficiency (k<sub>i</sub>) of the transport might be interpreted in the following way. The lower plasma-tyrosine concentration in the patients could be accompanied by an enhanced concentration of other amino acids, sharing the transport system with tyrosine. The net effect could be that the summed concentrations of the competing amino acids are the same for patients and controls. As k<sub>i</sub> should be determined by this total concentration, the two groups should then have similar k<sub>i</sub> values.

However, there is also another observation which cannot be explained by compensatory enhanced concentrations of other amino acids. Despite the similar tissue concentrations of tyrosine for the two groups, the net utilization rate was significantly lower for the patients than for controls.

Clearly, after 25 min there can be losses of labeled metabolites from the tissue, and there are metabolites in the plasma as well, facts which influence the determination of the net utilization rate. However, the important observation is the difference in the net utilization found between the two groups. The higher net utilization observed for controls suggests that both the loss of labeled metabolites and the fraction of labeled metabolites should be larger for controls compared to patients. In other words, after correction for losses from tissue and after correction for metabolites in plasma, differences in utilization of tyrosine between controls and patients should probably be larger than the difference obtained here with uncorrected data.

A striking feature of the data presented in Table 2 and Figure 2 is the small variation in the plasma concentration of tyrosine for the patients, which indicates per se a difference between the two groups.

Our interpretation of the data is that the observed differences between patients and controls combined indicate that tyrosine utilization is disturbed in patients with schizophrenia.

## ACKNOWLEDGMENTS

The authors thank the members of the PET group at Karolinska Institute in Stockholm, Ms. Kjerstin Lind and Alexandra Tylec for technical assistance, and Ms. Anita Liberg for preparing

the manuscript. This work was supported by grants from The Bank of Sweden Tercentenary Foundation and the Swedish Medical Research Council (08318).

## REFERENCES

- Pardridge WM, Oldendorf WH. Transport of metabolic substrates through the blood-brain barrier. *J Neurochem* 1977;28:5–12.
- Fernström JD, Faller DV. Neutral amino acids in the brain. Changes in response to food ingestion. *J Neurochem* 1978;30:1531–1538.
- Fernström JD. Role of precursor availability in control of monoamine biosynthesis in brain. *Phys Rev* 1983;63:484–546.
- Milner JD, Wurtman RJ. Catecholamine synthesis: physiological coupling to precursor supply. *Biochem Pharmacol* 1986;35:875–881.
- Hagenfeldt L, Bjerkenstedt L, Edman G, Sedvall G, Wiesel F-A. Amino acids in plasma and CSF and monoamine metabolites in CSF: interrelationship in healthy subjects. *J Neurochem* 1984;42:833–837.
- Bjerkenstedt L, Edman G, Hagenfeldt L, Sedvall G, Wiesel F-A. Plasma amino acids in relation to cerebrospinal fluid monoamine metabolites in schizophrenic patients and healthy controls. *Br J Psych* 1985;147:276–282.
- van Rossum JM. The significance of dopamine receptor blockade for the mechanism of action of neuroleptic drugs. *Arch Int Pharmacodyn Ther* 1966;160:492–494.
- Randrup A, Munkvad I. Brain dopamine and the amphetamine-reserpine interaction. *J Pharm Pharmacol* 1967;19:483–484.
- Carlsson A. Antipsychotic drugs, neurotransmitters, and schizophrenia. *Am J Psych* 1978;135:164–173.
- Hagenfeldt L, Venizelos N, Bjerkenstedt L, Wiesel F-A. Decreased tyrosine transport in fibroblasts from schizophrenic patients. *Life Sci* 1987;41:2749–2757.
- Bergström M, Boethius J, Eriksson L, Greitz T, Ribbe T, Widén L. Head fixation device for reproducible position alignment in transmission CT and positron emission tomography. *J Comput Assist Tomogr* 1981;5:136–141.
- Pennkopf E. *Atlas der topographischen und angewandten Anatomie des Menschen*. Erster Band: Kopf und Hals. 106. Munich: Urban und Schwarzenberg; 1963.
- Halldin L, Schoeps K-O, Stone-Elander S, Wiesel F-A. The Bücherer-Strecker synthesis of D- and L-[1-<sup>11</sup>C]tyrosine and the in vivo study of L-[<sup>11</sup>C]tyrosine in human brain using positron emission tomography. *Eur J Nucl Med* 1987;13:288–291.
- Beck O, Hesselgren T. Method for the determination of tryptophan in serum and cerebrospinal fluid. *J Chromatogr Biomed Appl* 1980;181:100–102.
- Eriksson L, Bohm C, Kesselberg M, Holte S. An automated blood sampling system used in positron emission tomography. *Nuclear Science Applications* 1988;3:133–143.
- Farde L, Eriksson L, Blomquist G, Halldin C. Kinetic analysis of central [<sup>11</sup>C]raclopride binding to D<sub>2</sub> dopamine receptors studied by PET—a comparison to the equilibrium analysis. *J Cereb Blood Flow Metab* 1989;9:696–708.
- Nilsson JLG, Stone-Elander S, Ehrin S, Garmelius B, Johnström P. Labelled compounds for the study of cerebral blood volume, blood flow, and energy metabolism. In: Greitz T, Ingvar D, Widén L, eds. *The metabolism of the human brain studied with positron emission tomography*. New York: Raven Press; 1985:107–112.
- Phelps ME, Huang SC, Hoffmann EG, Kuhl DE. Validation of tomographic measurement of cerebral blood volume with C-11-labelled carboxyhemoglobin. *J Nucl Med* 1979;20:328–334.
- Bradbury MWB, Patlak CS, Oldendorf WH. Analysis of brain uptake and loss of radiotracers after intracarotid injection. *Am J Physiol* 1975;229:1110–1115.
- Oldendorf WH. Brain uptake of radiolabelled amino acids, amines, and hexoses after arterial injection. *Am J Physiol* 1991;221:1629–1639.
- Crone C. The permeability of capillaries in various organs as determined by use of the “indicator diffusion” method. *Acta Physiol Scand* 1963;58:292–305.
- Ishiwata K, Vaalburg W, Elsinga PH, Paans AMJ, Woldring MG. Metabolic studies with L-(1-<sup>14</sup>C)tyrosine for the investigation of a kinetic model to measure protein synthesis rates with PET. *J Nucl Med* 1988;29:524–529.
- Sjöquist B, Mårdh G, Änggård E. Use of stable isotopes in studies on

- catecholamine metabolism in man. In: Yoshida H, ed. *Advances in pharmacology and therapeutics II*, volume 6. New York: Pergamon Press; 1982:221-226.
24. Blomqvist G. On the construction of functional maps in positron emission tomography. *J Cereb Blood Flow Metab* 1984;4:629-632.
  25. Patlak CS, Blasberg RG, Fenstermacher JD. Graphical evaluation of blood-to-brain transfer constants from multiple-time uptake data. *J Cereb Blood Flow Metab* 1983;3:1-7.
  26. Miller LP, Pardridge WM, Braun LD, Oldendorf WH. Kinetic constants for blood-brain barrier amino acid transport in conscious rats. *J Neurochem* 1985;45:1427-1432.
  27. O'Tuama LA, Guijarro TR, Douglas KH et al. Assessment of [<sup>11</sup>C]-L-methionine transport into the human brain. *J Cereb Blood Flow Metab* 1988;8:341-345.

(continued from page 5A)

## FIRST IMPRESSIONS

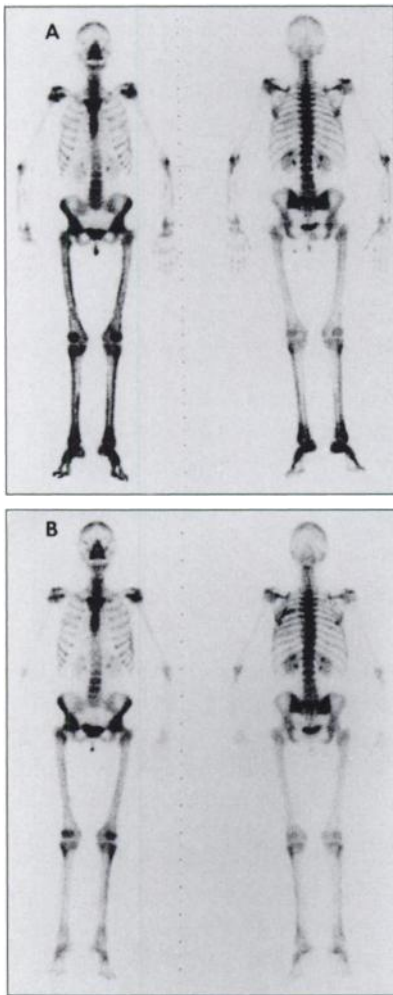


**FIGURE 1.** (A) Bone scintigraphy June 1990. (B) Bone scintigraphy October 1990.

### ACQUISITION INFORMATION

A 44-yr-old female with a bronchogenic carcinoma suffered from severe pain in both ankles and feet and also in both wrists and hands. Physical examination essentially revealed clubbing of the fingers as well as swelling, painful palpation and erythema of the calves and ankles. The first <sup>99m</sup>Tc-MDP bone scan showed a symmetrical increased tracer uptake along the cortical margins of the long bones of the appendicular skeleton, especially in its distal parts. This finding, together with the clinical picture, was highly suggestive for hypertrophic pulmonary osteoarthropathy (HPO). Since no metastatic lesions were found, the patient underwent a left pneumectomy. The pain in her extremities decreased rapidly. A clinical history can be deduced from the follow-up bone scan findings: the hyperactive lesion at the posterior part of the left fifth rib corresponds to the site of the surgical intervention; the scintigraphic signs of HPO had almost completely disappeared.

### TRACER

20 mCi of <sup>99m</sup>Tc-MDP

### ROUTE OF ADMINISTRATION

Intravenous injection

### TIME AFTER INJECTION

Three hours

### INSTRUMENTATION

Siemens Body Scan

### CONTRIBUTORS

A. Jacobs, A. Bossuyt, and M.H. Jonckheer

### INSTITUTION

Department of Nuclear Medicine, AZ-VUB, Brussels, Belgium